

Fano effect on Josephson current

This article has been downloaded from IOPscience. Please scroll down to see the full text article.

2005 J. Phys.: Condens. Matter 17 4637

(<http://iopscience.iop.org/0953-8984/17/29/006>)

View [the table of contents for this issue](#), or go to the [journal homepage](#) for more

Download details:

IP Address: 129.252.86.83

The article was downloaded on 28/05/2010 at 05:38

Please note that [terms and conditions apply](#).

Fano effect on Josephson current

Zhi-Yong Zhang

Department of Physics, Nanjing University, Nanjing 210093, People's Republic of China

Received 10 March 2005, in final form 10 June 2005

Published 8 July 2005

Online at stacks.iop.org/JPhysCM/17/4637

Abstract

We investigate the influence of the Fano effect on the Josephson current through a quantum dot (QD) coupled to two identical superconductors (SCs). Our attention is focused on the situation where the Kondo spin singlet survives the superconductivity and the finite- U slave-boson mean-field method is adopted to treat the Kondo correlation. With the direct coupling between the two SCs increased, the Josephson current varies in different manners in different regimes. This is consistent with the variation of Josephson coupling, which exhibits characteristics similar to those shown by the conductance through a QD connected to normal leads. But unlike the normal conductance, a negative Josephson coupling region is formed in the dip of the characteristic asymmetric peak–dip structure. Accompanying this $0\text{--}\pi$ transition, a new kind of intermediate states is found, which are different from those caused by effective ferromagnetic interaction. This $0\text{--}\pi$ transition and the intermediate states are yielded entirely by the Fano effect.

1. Introduction

The quantum interference effect plays an important role in the mesoscopic physics. When a discrete energy level is embedded in a continuum energy state, the quantum interference between two configurations—one through the resonant level and the other directly through the continuum—leads to the Fano effect [1], a ubiquitous phenomenon first found in atomic physics then in other areas [2–4], which is characterized by an asymmetric line shape. Because of its tunability, quantum dot (QD) systems have attracted a lot of attention. When a dot is connected to normal metallic leads, the coupling between the localized spin on the dot and conduction electrons leads to the Kondo correlation, which is described by an energy scale T_K , the so-called Kondo temperature. When a QD is in the Kondo regime [5–9], the localized spin and conduction electrons forms a spin singlet state, which yields the Abrikosov–Suhl resonance and profoundly affects the electronic transport. If the Fano effect is introduced in a QD system, the Fano–Kondo effect, frequency doubling of Aharonov–Bohm (AB) oscillation and pinning of the AB maximum are found [10–13].

When a barrier is sandwiched between two identical superconductors (SCs), a Josephson current J can be yielded by the phase difference φ between the two SCs. When the tunnelling

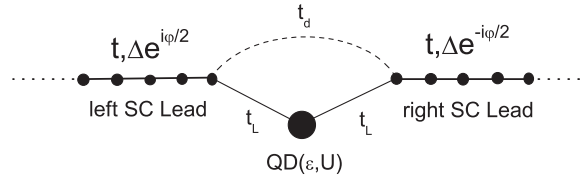


Figure 1. Schematic illustration of the structure.

through the barrier is weak and conserves spin, the Josephson current can be expressed as $J = J_c \sin(\varphi)$, where the Josephson coupling J_c is proportional to the normal conductance through the barrier. But if the barrier is ferromagnetic, negative Josephson coupling is found [14]. Embedding a QD in between two SCs results in competition between the Kondo effect and superconductivity at low temperature [15, 16]. With T_K smaller than the superconducting gap Δ , the Kondo spin singlet is broken, which leads to negative J_c or π -junction. With $T_K > \Delta$, the Josephson current is enhanced by the Kondo effect and the Josephson coupling is positive (0-junction). In the intermediate regime, a ‘0’ or ‘ π ’ junction can be found according to the location of the global minimum of the bound state energy being at 0 or π [17–24]. Now, it is natural to ask how the Fano effect influences the Josephson current if the two SCs are coupled by direct tunnelling.

In the present paper, we focus our attention on the situation where $T_K > \Delta$ and the Kondo singlet survives the superconductivity. Our purpose is to answer the following four questions. (i) Does the Fano effect influence J in the same manner in different regimes? (ii) If not, what is the underlying rule? (iii) Can the Fano effect yield the $0-\pi$ transition and corresponding intermediate states? (iv) If it can, how about the relationship between this kind of transition and that caused by the effective ferromagnetic interaction? To this purpose, we assume a structure illustrated schematically in figure 1, describe the superconductivity in the BCS scheme and adopt the finite- U slave-boson mean-field theory (f - U SBMFT) [25, 26] to treat the Kondo correlation. As we know from the previous studies [20–22], the SBMFT can give qualitative correct results when $T_K > \Delta$. With the direct coupling between the two SCs increased, the Josephson current varies in different manners in different regimes. This is consistent with the variation of Josephson coupling, which exhibits characteristics similar to those of the conductance through a QD connected to normal leads and shows an asymmetric line shape, the universal characteristic of the Fano effect. But unlike the normal conductance, an NJC region is formed in the dip of the asymmetric peak–dip structure. At the edges of the NJC region, a new kind of intermediate states is found. They are different from the ‘0’ and ‘ π ’ states caused by the competition between the Kondo effect and superconductivity. This kind of $0-\pi$ transition and the associated intermediate states are yielded entirely by the Fano effect. The existence of an NJC region is a special characteristic of the Fano effect in Josephson junctions, and the Fano effect is an important way leading to the π -junction, parallel with that through the effective ferromagnetic interaction.

The organization of this paper is as follows. In section 2, the theoretical model and calculation method are illustrated. In section 3, the numerical results and discussion on them are presented. A brief summary is given in section 4.

2. Model and formulae

In the present paper, we investigate the influence of the Fano effect on the Josephson current through a QD, which is coupled to two SCs. The structure is schematically illustrated in figure 1,

where one dot, with a single-particle energy level ϵ_d and an on-site Coulomb interaction U , is connected to SCs by hopping integral t_L . Here, the two SCs are assumed entirely identical except for a phase difference φ , and without loss of generality it is assumed that $\varphi_L = -\varphi_R = \varphi/2$. The two SCs are also coupled directly with each other by a tunnelling matrix element t_d . Employing the BCS theory to deal with the SCs, we describe this mesoscopic system by the following 1D tight-binding Hamiltonian:

$$H = H_L + H_R + H_D + H_T, \quad (1)$$

where H_j ($j = L, R$) H_D and H_T are the Hamiltonians of the leads, the dot and the coupling between them, respectively. They are

$$H_L = - \sum_{i=-\infty}^{-1} \left\{ t \sum_{\sigma} c_{i-1,\sigma}^{\dagger} c_{i,\sigma} + \Delta e^{i\varphi/2} c_{i,\uparrow}^{\dagger} c_{i,\downarrow}^{\dagger} + \text{H.c.} \right\}, \quad (2)$$

$$H_R = - \sum_{i=1}^{\infty} \left\{ t \sum_{\sigma} c_{i,\sigma}^{\dagger} c_{i+1,\sigma} + \Delta e^{-i\varphi/2} c_{i,\uparrow}^{\dagger} c_{i,\downarrow}^{\dagger} + \text{H.c.} \right\}, \quad (3)$$

$$H_D = \epsilon_d \sum_{\sigma} c_{0,\sigma}^{\dagger} c_{0,\sigma} + U n_{0,\uparrow} n_{0,\downarrow} \quad (4)$$

and

$$H_T = - \sum_{\sigma} \left\{ t_L (c_{-1,\sigma}^{\dagger} + c_{1,\sigma}^{\dagger}) c_{0,\sigma} + t_d c_{1,\sigma}^{\dagger} c_{-1,\sigma} + \text{H.c.} \right\}. \quad (5)$$

Here $n_{0,\sigma} = c_{0,\sigma}^{\dagger} c_{0,\sigma}$, with $\sigma = \uparrow$ or \downarrow .

The normal state Kondo temperature T_K is given by $T_K = \frac{U\sqrt{J_K}}{2\pi} \exp(-\pi/J_K)$ [27], with $J_K = \frac{-2U\Gamma}{\epsilon_d(\epsilon_d+U)}$. Here, with the Fermi energy being set as zero, the hybridization strength $\Gamma = 2t_L^2/t$ (cf [28]) and the correlation length of the spin singlet $\xi_K = 2t/T_K$ at zero temperature. In the present paper, we are interested in the situation where $T_K > \Delta$ and the Kondo singlet state survives the superconductivity. As we know from the previous studies [20–22], in that regime, treating the Kondo correlation with the slave-boson mean-field theory (SBMFT) can give qualitatively correct results. Here, the finite- U SBMFT of Kotliar and Ruckenstein (KR) [25, 26] is adopted. In the framework of this approach, four auxiliary boson fields e , p_{σ} and d are introduced, which act as projection operators onto the empty, singly occupied and doubly occupied electronic states at the dot. To eliminate the unphysical states, three constraints are imposed: $\sum_{\sigma} p_{\sigma}^{\dagger} p_{\sigma} + e^{\dagger} e + d^{\dagger} d = 1$ and $n_{0,\sigma} = p_{\sigma}^{\dagger} p_{\sigma} + d^{\dagger} d$. To obtain the correct result in the noninteracting limit, the fermion operator $c_{0,\sigma}$ should be replaced by $c_{0,\sigma} z_{\sigma}$, with $z_{\sigma} = (1 - d^{\dagger} d - p_{\sigma}^{\dagger} p_{\sigma})^{-1/2} (e^{\dagger} p_{\sigma} + p_{\sigma}^{\dagger} d) (1 - e^{\dagger} e - p_{\sigma}^{\dagger} p_{\sigma})^{-1/2}$. Therefore the Hamiltonian (1) can be replaced by the following effective Hamiltonian:

$$H_{\text{eff}} = H_L + H_R + \tilde{H}_D + \tilde{H}_T + \lambda^{(1)} \left(\sum_{\sigma} p_{\sigma}^{\dagger} p_{\sigma} + e^{\dagger} e + d^{\dagger} d - 1 \right) + \sum_{\sigma} \lambda_{\sigma}^{(2)} (n_{0,\sigma} - p_{\sigma}^{\dagger} p_{\sigma} - d^{\dagger} d), \quad (6)$$

where the three constraints are incorporated by the three Lagrange multipliers $\lambda^{(1)}$ and $\lambda_{\sigma}^{(2)}$. Here, the original H_D and H_T are replaced by

$$\tilde{H}_D = \epsilon_d \sum_{\sigma} c_{0,\sigma}^{\dagger} c_{0,\sigma} + U d^{\dagger} d \quad (7)$$

and

$$\tilde{H}_T = - \sum_{\sigma} \left\{ t_L (c_{-1,\sigma}^{\dagger} + c_{1,\sigma}^{\dagger}) c_{0,\sigma} z_{\sigma} + t_d c_{1,\sigma}^{\dagger} c_{-1,\sigma} + \text{H.c.} \right\}. \quad (8)$$

To solve the effective Hamiltonian (6) at zero temperature, we first replace the slave boson fields by their expectation values, then obtain the values of e , p_σ , d , $\lambda^{(1)}$ and $\lambda_\sigma^{(2)}$ by minimization of the ground state energy E_0 of the essentially noninteracting Hamiltonian (6) with respect to these parameters [26]. This is equivalent to the approach using the functional integral method combined with the saddle-point approximation, and leads to a set of self-consistent equations [25, 26]:

$$\sum_{\sigma} p_{\sigma}^2 + e^2 + d^2 = 1, \quad (9)$$

$$\langle 0|n_{0,\sigma}|0\rangle = p_{\sigma}^2 + d^2, \quad (10)$$

$$-t_L \sum_{\sigma} \text{Re} \left\{ \langle 0|(c_{-1,\sigma}^{\dagger} + c_{1,\sigma}^{\dagger})c_{0,\sigma}|0\rangle \right\} \frac{\partial z_{\sigma}}{\partial e} + \lambda^{(1)}e = 0, \quad (11)$$

$$-t_L \sum_{\sigma'} \text{Re} \left\{ \langle 0|(c_{-1,\sigma'}^{\dagger} + c_{1,\sigma'}^{\dagger})c_{0,\sigma'}|0\rangle \right\} \frac{\partial z_{\sigma'}}{\partial p_{\sigma}} + \lambda^{(1)}p_{\sigma} - \lambda_{\sigma}^{(2)}p_{\sigma} = 0, \quad (12)$$

and

$$\sum_{\sigma} \left\{ -t_L \text{Re}[\langle 0|(c_{-1,\sigma}^{\dagger} + c_{1,\sigma}^{\dagger})c_{0,\sigma}|0\rangle] \frac{\partial z_{\sigma}}{\partial d} - \lambda_{\sigma}^{(2)}d \right\} + \lambda^{(1)}d + Ud = 0. \quad (13)$$

To self-consistently solve these equations, we have to calculate the expectation values such as $\langle 0|c_{j,\sigma}^{\dagger}c_{i,\sigma}|0\rangle$, with $|0\rangle$ the ground state corresponding to a certain set of variational parameters, then update the variational parameters from the above self-consistent equations, and repeat these two steps until numeric convergence is reached. If a quasiparticle wavefunction is expressed as $\alpha^{\dagger}|F\rangle = \sum_i (u_i c_{i,\uparrow}^{\dagger} - v_i c_{i,\downarrow})|F\rangle$ with $|F\rangle$ the Fermi sea, acting as a background, whose intrinsic structure is irrelevant with our calculation, the corresponding Schrödinger equation can be diagonalized to obtain a series of excited eigenstates, $\{\alpha_n^{\dagger}|F\rangle\}$. $c_{i,\uparrow}^{\dagger}$ and $c_{i,\downarrow}$ can be expressed by the quasiparticle operators $\{\alpha_n^{\dagger}\}$ and $\{\bar{\alpha}_n\}$. Here, $\bar{\alpha}_n^{\dagger}|F\rangle = \sum_i (u_{i,n} c_{i,\downarrow}^{\dagger} + v_{i,n} c_{i,\uparrow})|F\rangle$, the spin degenerate state with $\alpha_n^{\dagger}|F\rangle$. Because $|0\rangle$ is a state with no quasiparticle excited, the expectation value of $\langle 0|c_{j,\sigma}^{\dagger}c_{i,\sigma}|0\rangle$ can be written as: $\langle 0|c_{j,\sigma}^{\dagger}c_{i,\sigma}|0\rangle = \sum_n v_{j,n}^* v_{i,n}$. Generally, those expectation values can be analytically expressed in terms of variational parameters with the help of the Nambu representation and the Green-function technique [23, 29, 30], but the expressions are complex and tedious when t_d is introduced, and we prefer direct diagonalization. In practical calculation, the numeric diagonalization can be performed only in a finite cluster. (Here, the QD is located at the centre of the cluster.) If the cluster size is much larger than the coherence length ξ_K of the singlet state, the results obtained from the cluster calculation are identical with those from the original system [31, 32].

Due to the spin degeneracy, only five variational parameters should be determined. They are e , p , d , $\lambda^{(1)}$ and $\lambda^{(2)}$. As soon as the five variational parameters are determined, the eigenenergies and the corresponding wavefunctions of Andreev bound states can be obtained. At zero temperature, the Josephson current can be expressed as:

$$J(\varphi) = \frac{2}{\Delta} \sum_{\lambda} \frac{\partial E_{\lambda}(\varphi)}{\partial \varphi} = 2 \text{Im} \sum_{\lambda} \left\{ e^{i\varphi/2} \sum_{i=-\infty}^{-1} \langle \lambda|c_{i,\uparrow}^{\dagger}c_{i,\downarrow}^{\dagger}|\lambda\rangle - e^{-i\varphi/2} \sum_{i=1}^{\infty} \langle \lambda|c_{i,\uparrow}^{\dagger}c_{i,\downarrow}^{\dagger}|\lambda\rangle \right\}. \quad (14)$$

Here, $\langle \lambda|c_{i,\uparrow}^{\dagger}c_{i,\downarrow}^{\dagger}|\lambda\rangle = v_{i,\lambda}^* u_{i,\lambda}$, with $|\lambda\rangle$ an Andreev bound state below the Fermi level and E_{λ} the corresponding eigenenergy.

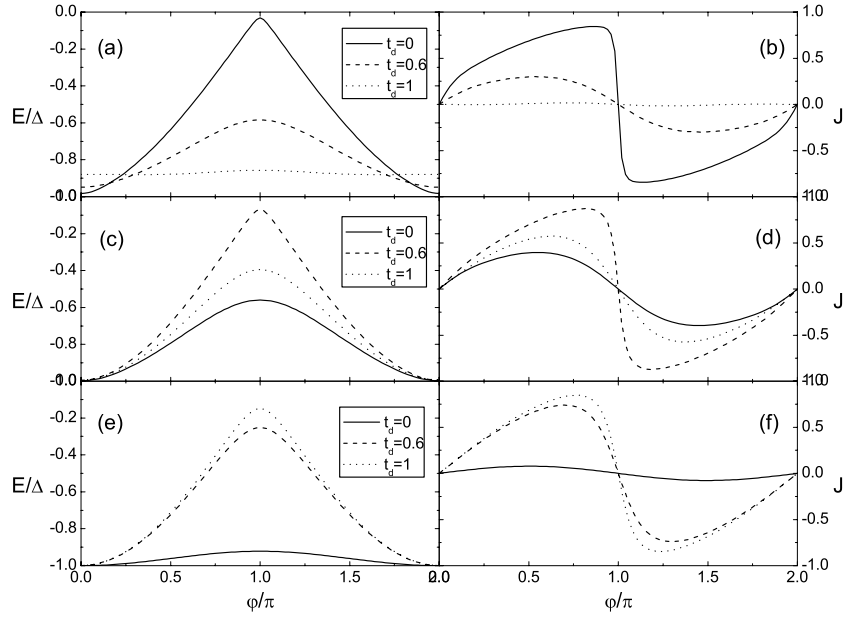


Figure 2. E - φ and J - φ curves for different t_d with $\epsilon_d = -0.7$ ((a) and (b)), $\epsilon_d = 0$ ((c) and (d)) and $\epsilon_d = 0.7$ ((e) and (f)). Here, solid lines correspond to $t_d = 0$, dashed 0.6 and dotted 1. The other parameters are $t = 1$, $t_L = 0.4$, $U = 1.4$ and $\Delta = 0.04$.

3. Results and discussion

In the following calculation, we always set $t = 1$, $t_L = 0.4$, $U = 1.4$ and $\Delta = 0.04$ except in figure 5(b). At the particle-hole symmetric point $\epsilon_d = -U/2$, the Kondo temperature of the normal state $T_K = 0.0541$ and the corresponding coherent length $\xi_K = 37.0$. Here, Δ is smaller than T_K . Generally, the effective Kondo temperature with $t_d \neq 0$ is always larger than Δ in our SBMFT calculation, and in our numeric diagonalization the cluster size is set as 300, which can guarantee the numeric convergence even if $t_d = 1$.

In figure 2, the variations of bound state energy E below the Fermi level and Josephson current J with φ are presented for different t_d . Here, the subscript λ of E is omitted because of the spin degeneracy. The E - φ curve corresponding to the bound state above the Fermi level is symmetric with the plotted one. The quantum interference effect influences E and J in different manners when the QD is in different regimes, but E and J exhibit similar variation trend at the same ϵ_d . When $\epsilon_d = -0.7$, the oscillation amplitudes of E - φ and J - φ curves are suppressed by the Fano effect and the shape of the J - φ curve becomes more sinusoidal. The situation with $\epsilon_d = 0.7$ is just the opposite: the oscillation amplitudes are increased and the shape of J - φ curves is more sawtooth-like. In the mixed-valence regime with $\epsilon_d = 0$, the oscillation amplitudes are first increased then suppressed. Generally, with these three ϵ_d , the energy minimum of the bound state is located at $\varphi = 0$, associated with positive Josephson coupling, which corresponds to the so-called 0 junction. But an exception exists at $\epsilon_d = -0.7$ with $t_d = 1$ where the bound state minimum is removed from $\varphi = 0$ and $J \propto -\varphi$ around $\varphi = 0$. (The corresponding E - φ and J - φ curves are given separately in figures 4(c) and (d).) This exception implies a 0- π transition caused by the Fano effect.

These results are consistent with the characteristics shown by the E_c - ϵ_d and J_c - ϵ_d curves. Here, E_c and J_c are defined as $E(\varphi = \pi/2)$ and $J(\varphi = \pi/2)$, respectively. They are plotted

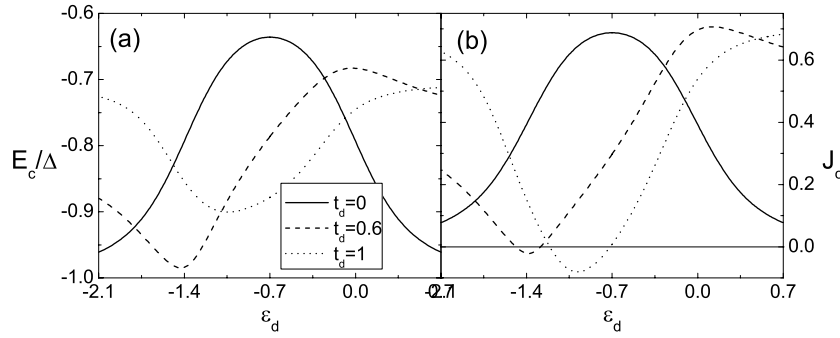


Figure 3. $E_c - \epsilon_d$ (a) and $J_c - \epsilon_d$ (b) curves for $t_d = 0$ (solid), 0.6 (dashed) and 1 (dotted). The other parameters are the same as in figure 2.

in figure 3 for different t_d . These two types of curves exhibit characteristics similar to those shown by the conductance through a QD connected to normal metallic leads. When $t_d = 0$, a high plateau appears in the regime $[-U, 0]$, and with $|\epsilon_d + U/2| \gg \Gamma$, E_c approaches $-\Delta$ whereas J_c approaches zero. With the Fano effect introduced the plateau is replaced by a peak-dip structure in both of the two curves, and with $|\epsilon_d + U/2| \gg \Gamma$ both E_c and J_c are enhanced. In the normal conductance, a Fano-Kondo plateau is sandwiched in between peak and dip, but in the E_c and J_c curves, because of the relatively large Γ , the Fano-Kondo plateau is merged into the peak-dip structure. When $t_d = 1$ (the normal transmissivity through the direct channel is unity) a low plateau appears in the regime $[-U, 0]$, and outside that regime E_c and J_c are further enhanced. These account for the different variation trends of the $E-\varphi$ and $J-\varphi$ curves in different regimes.

The asymmetric line shape is a universal characteristic of the Fano effect, and in Josephson junctions this is shown in the $E_c - \epsilon_d$ and $J_c - \epsilon_d$ curves. On the other hand, as we have said in the introduction, the Josephson coupling J_c is proportional to the normal conductance only if the tunnelling process is weak and conserves spin. Although J_c exhibits characteristics similar to those of the normal conductance, the difference between them is remarkable. The most striking is the appearance of a negative Josephson coupling region. (In figure 3(b), a thin horizontal line indicates the position where $J_c = 0$.) This region always exists in the dip or low plateau with $t_d \neq 0$. Because the appearance of an NJC region is a special characteristic of Josephson junctions with the Fano effect, we focus our attention on its properties in the following.

In figure 4, the $E-\varphi$ and $J-\varphi$ curves are given at $\epsilon_d = -0.7$ and -0.98 with $t_d = 1$. With $\epsilon_d = -0.98$, the minimum of the bound state energy is located at $\varphi = \pi$, and around $\varphi = 0$, $J \propto -\varphi$. This is a clear demonstration of the $0-\pi$ transition caused by the Fano effect: if the SC leads are connected into a ring, at zero temperature, the ground state is at the π state and the ring is threaded through with half a flux quantum because of the flux quantization. The situation with $\epsilon_d = -0.7$ is subtle: it is close to but outside the NJC region (cf figure 3(b)). The maximum of bound state energy is still located at $\varphi = \pi$, but now the minimum is moved away from $\varphi = 0$, and two identical minima appear symmetrically with $\varphi = \pi$. Around $\varphi = 0$, J is also $\propto -\varphi$, like a junction with negative Josephson coupling, but with φ further increased the absolute value of J decreases and then its sign is changed before $\varphi = \pi/2$. The subsequent behaviour of J is somewhat sinusoidal, like a junction with positive Josephson coupling. This corresponds to an intermediate state. With ϵ_d entering the NJC region, the two minima move towards each other until they coincide at $\varphi = \pi$ where the structure is

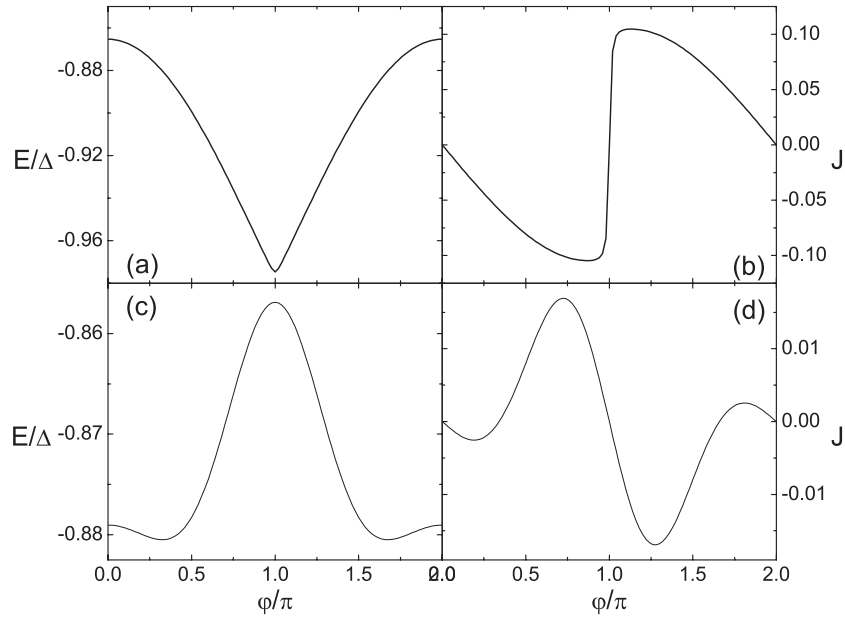


Figure 4. E - φ and J - φ curves for $\epsilon_d = -0.98$ ((a) and (b)) and -0.7 ((c) and (d)) with $t_d = 1$. The other parameters are the same as in figure 2.

altered into a π -junction. Unlike the ‘0’ and ‘ π ’ states coming from the competition between the Kondo effect and superconductivity [17–24], the appearance of the two minima is not the result of the crossing of different bound energy levels, and no kink is found in the E or J curves. This kind of 0 - π transition and the accompanied intermediate states are peculiar to the Fano effect.

This point can be further clarified by investigating the J_c - ϵ_d curves in the situation with $U = 0$, which are given in figure 5(a) for different t_d . When $t_d = 0$, the Andreev reflection causes a resonant peak at $\epsilon_d = \epsilon_F = 0$ with the peak width being 2Γ . When $t_d = 0.6$ the quantum interference between the path through the dot and the direct path leads to a peak-dip structure, and with $t_d = 1$ a dip structure is left. These results are also similar to those of the corresponding normal conductance, and the asymmetric line shape of the J_c - ϵ_d curve reflects the universal characteristic of the Fano effect. As in the situation with $U \neq 0$, an NJC region is formed in the dip when $t_d \neq 0$, and intermediate states similar to those with $U \neq 0$ can be found at the edges of the NJC region (not presented here). The 0 - π transition is entirely yielded by the Fano effect no matter whether there is a Kondo correlation or not, and the appearance of the NJC region is a special characteristic of the Fano effect when Josephson junctions are concerned. Comparing figures 3(b) and 5(a), we can see that the main effect of the Kondo correlation is to change the position and extent of the NJC region. Despite the mean-field nature of the f - U SBMFT, the existence of this new kind of 0 - π transition should be independent of which method is taken to treat the Kondo correlation. Even if the Kondo correlation is overwhelmed by the superconductivity, the Fano effect is still an important way leading to the 0 - π transition, parallel with that through the effective ferromagnetic interaction.

As we have said at the beginning of this section, the preceding results are all obtained with fixed $t_L = 0.4$ and $\Delta = 0.04$. To generalize the above results, in figure 5(b), $\ln(-J_c^{(s)}/\Delta^2) - \ln(t_d/t_L)$ curves are plotted for different Δ and t_L , with $J_c^{(s)}$ the tip value of

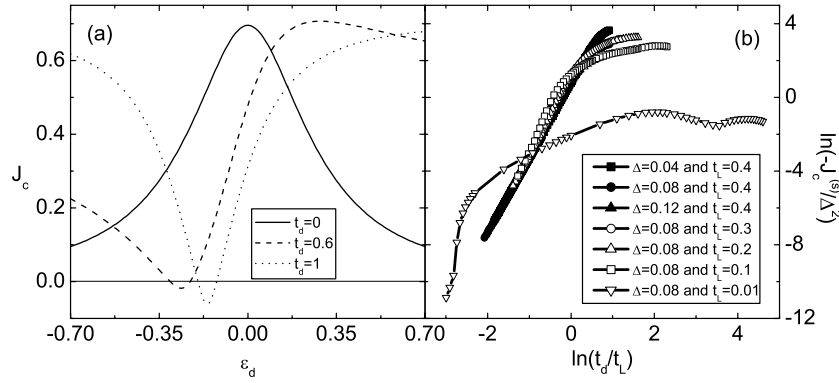


Figure 5. (a) J_c - ϵ_d curves for $t_d = 0$ (solid), 0.6 (dashed) and 1 (dotted). The other parameters are $t = 1$, $t_L = 0.4$, $U = 0$ and $\Delta = 0.04$. (b) $\ln(-J_c^{(s)}/\Delta^2) - \ln(t_d/t_L)$ curves for different Δ and t_L with $t = 1$ and $U = 0$.

the J_c dip. (Here, Δ should be understood as Δ/t , a dimensionless parameter.) For simplicity of the calculation, these results are obtained with $U = 0$. When $t_L = 0.4$ and $\Delta = 0.04$, the curve is approximately a straight line $\ln(-J_c^{(s)}/\Delta^2) = 4 \ln(t_d/t_L) + c$ with c a fit parameter, which is small but not zero, and the curve deviates from the line only in the part where t_d is close to unity, corresponding to the right end of the curve. (The range of $\ln(t_d/t_L)$ is from $-\infty$ to $\ln(1/t_L)$ for a certain t_L .) With t_L fixed, increasing Δ extends the area of that deviation, where the curve becomes flat and lowered. In the range of Δ we take (from 0.04 to 0.12) this variation is mild. A similar variation is also found when decreasing t_L with Δ fixed. When $\Delta = 0.08$, with t_L decreased from 0.4 to 0.2, this kind of variation is small; with $t_L = 0.1$, the variation is noticeable, and with $t_L = 0.01$, it is prominent. Despite the extension of the deviation, with $\ln(t_d/t_L) \rightarrow -\infty$, the curve always approaches the straight line, and with larger Δ or lower t_L that limit can only be reached with larger $|\ln(t_d/t_L)|$. This point can be seen clearly from the curve with $\Delta = 0.08$ and $t_L = 0.01$. These observations are consistent with our intuitive picture and further confirm the applicability of our approximation scheme.

If a magnetic flux is threaded through the area enclosed by the two paths, Josephson current can flow through the structure even if the phase difference between the two SCs disappears. Like the normal conductance, the doubling of the Aharonov-Bohm (AB) oscillation frequency and the ‘pinning’ of the AB maximum are found in the J_c curves, which reflects the universal characteristics of the Fano effect. On the other hand, as a special characteristic of the Fano effect in Josephson junctions, an NJC region can still be found when an external magnetic flux is introduced. These results can be expected from the perspective obtained in the preceding paragraphs and our knowledge on the conductance through normal leads, and their details are not given here.

4. Summary

In summary, we investigate the influence of the Fano effect on the Josephson current through a QD in the situation where $T_K > \Delta$ and deal with the Kondo correlation by the f - U SBMFT. With the direct coupling between the two SCs introduced and increased, the Josephson current varies in different manners in different regimes. This is consistent with the variation of Josephson coupling, which exhibits characteristics similar to those of the conductance through a QD connected to normal leads and shows an asymmetric line shape, the universal

characteristic of the Fano effect. But unlike the normal conductance, an NJC region is formed in the dip of the asymmetric peak–dip structure. Accompanied by this $0\text{--}\pi$ transition, a new kind of intermediate states is found at the edges of the NJC region, which is different from those caused by the effective ferromagnetic interaction. This kind of $0\text{--}\pi$ transition and the associated intermediate states can be found even when $U = 0$. They are yielded entirely by the Fano effect, and the existence of an NJC region is a special characteristic of the Fano effect in Josephson junctions. The Fano effect is an important way leading to the π -junction, parallel with that through the effective ferromagnetic interaction.

Acknowledgments

The author acknowledges the support by National Foundation of Natural Science in China, grant No 10204012, and by the special funds for Major State Basic Research Project No G001CB3095 of China.

References

- [1] Fano U 1961 *Phys. Rev.* **124** 1866
- [2] Göres J *et al* 2000 *Phys. Rev. B* **62** 2188
- [3] Zacharia I G *et al* 2001 *Phys. Rev. B* **64** 155311
- [4] Kobayashi K, Aikawa H, Katsumoto S and Iye Y 2002 *Phys. Rev. Lett.* **88** 256806
- [5] Goldhaber-Gordon D, Shtrikman H, Mahalu D, Abusch-Magder D, Meirev U and Kaster M A 1998 *Nature* **391** 156
- [6] Cronewett S M, Oosterkamp T H and Kouwenhoven L P 1998 *Science* **281** 540
- [7] Simmel F, Blick R H, Kotthaus U P, Wegscheider W and Blichler M 1999 *Phys. Rev. Lett.* **83** 804
- [8] van der Wiel W G, De Franceschi S, Fujisawa T, Elzerman J M, Tarucha S and Kouwenhoven L P 2000 *Science* **289** 2105
- [9] Ji Y, Heiblum M, Sprinzak D, Mahalu D and Shtrikman H 2000 *Science* **290** 779
- [10] Hofstetter W, König J and Shoeller H 2001 *Phys. Rev. Lett.* **87** 156803
- [11] Bulka B R and Stefanski P 2001 *Phys. Rev. Lett.* **86** 5128
- [12] Kang K, Cho S Y, Kim J J and Shin S C 2001 *Phys. Rev. B* **63** 113304
- [13] Franco R, Figueira M S and Anda E V 2003 *Phys. Rev. B* **67** 155301
- [14] Kulik I O 1966 *Sov. Phys.—JETP* **22** 841
- [15] Buitelaar M R, Nussbaumer T and Schönenberger C 2002 *Phys. Rev. Lett.* **89** 256801
- [16] Buitelaar M R, Belzig W, Nussbaumer T, Babic B, Bruder C and Schönenberger C 2003 *Phys. Rev. Lett.* **91** 057005
- [17] Shiba H and Soda T 1969 *Prog. Theor. Phys.* **41** 25
- [18] Glazman L I and Matveev K A 1988 *Pis. Zh. Tekh. Fiz.* **49** 570
Glazman L I and Matveev K A 1989 *JETP Lett.* **49** 659 (Engl. Transl.)
- [19] Spivak B I and Kivelson S A 1991 *Phys. Rev. B* **43** 3740
- [20] Rozhkov A V and Arovas D P 1999 *Phys. Rev. Lett.* **82** 1788
- [21] Clerk A A and Ambegaokar V 2000 *Phys. Rev. B* **61** 9109
- [22] Rozhkov A V and Arovas D P 2000 *Phys. Rev. B* **62** 6687
- [23] Vecino E, Martin-Rodero A and Levy Yeyati A 2003 *Phys. Rev. B* **68** 035105
- [24] Choi M-S, Lee M, Kang K and Belzig W 2004 *Phys. Rev. B* **70** 020502
- [25] Kotliar G and Ruckenstein A E 1986 *Phys. Rev. Lett.* **57** 1362
- [26] Dorin V and Schlottmann P 1993 *Phys. Rev. B* **47** 5095
- [27] Hewson A C 1993 *The Kondo Problem to Heavy Fermions* (Cambridge: Cambridge University Press)
- [28] Kang K and Shin S-C 2000 *Phys. Rev. Lett.* **85** 5619
- [29] Avishai Y, Golub A and Zaikin A D 2001 *Phys. Rev. B* **63** 134515
Avishai Y, Golub A and Zaikin A D 2003 *Phys. Rev. B* **67** 041301
- [30] Golub A and Avishai Y 2004 *Phys. Rev. B* **69** 165325
- [31] Affleck I and Simon P 2001 *Phys. Rev. Lett.* **86** 2854
- [32] Hu H, Zhang G-M and Yu L 2001 *Phys. Rev. Lett.* **86** 5558